A Two-Dimensional Numerical Solution of Transient Magnetic Flux Distribution in Electric Machines Considering Magnetic Saturation and Hysteresis

By

Tsuguo ANDO* and Juro UMOTO*

(Received March 28, 1986)

Abstract

In recent electric machines, it is needed to analyse the transient behaviors of the magnetic fluxes which relate closely to the dynamic characteristics. In this paper, first, there are introduced two-dimensional fundamental equations with respect to the vector potential from the Maxwell equations in the electro-magnetic field. Here, the vector potential is used to easily obtain both the transient magnetic flux and the eddy current distributions in the electric machines. In order to solve numerically the above fundamental equations, the nodal equation at each node of the triangular meshes, by which the region to be analysed is subdivided, is obtained by a new nodal method, which is an improvement over the conventional nodal method by using any shape of the triangle. Next, the time derivative of the vector potential in the nodal equation, which is needed to calculate the eddy current, is approximated by the Crank-Nikolson finite difference method. Also, the authors show a numerical method for deriving the nonlinear reciprocal permeabilities from the magnetization and the hysteresis curves of the structural iron cores of the electric machines, in which the Frölich formula is used. Furthermore, from every nodal equation with the above approximated time derivative and the boundary conditions, the final fundamental nonlinear simultaneous nodal equations are derived. Lastly, the calculation processes to solve numerically the nodal equations are shown.

1. Introduction

In recent electric machines, it is very important to maintain the good dynamic characteristics in the transient state where the currents in the exciting windings change abruptly, and the eddy currents are induced in the structural iron cores. Then, it is needed to analyse precisely the transient behaviors of the magnetic fluxes which relate closely to the dynamic characteristics. Here, as is well known, the magnetic fluxes and the currents are perpendicularly linked to each other, and the approximate mag-

* Department of Electrical Engineering

netic fluxes can be obtained by the two-dimensional analysis in the cross-section to the effective current direction. Hitherto, there were many studies on the two-dimensional analyses of transient magnetic fluxes. However, those studies were mostly carried out by the analytical method of separation of variables on the assumption that the magnetic circuit of the electric machine can be simulated by a simplified magnetic circuit model with some constant permeabilities[1]-[4].

Now, the actual electric machine has iron cores with nonlinear permeabilities, which are caused by the magnetic saturation and the hysteresis, and the complicatedly shaped configuration. It is thought that these factors have much influence on the transient magnetic fluxes. In order to take these factors into consideration, two-dimensional numerical solutions, to which the finite difference, the finite element methods, etc. are applied, should be used.

The finite difference method[5],[6], in which the physical law about magnetic fluxes can be approximated at any grid of the rectangular meshes, is difficult to apply to the complicatedly shaped magnetic circuit of the electric machine. The finite element method[7], in which arbitray triangular meshes are usually used and the variational principle is used to approximate the physical law at each node of the meshes, has the flexibility to be able to be applied to the complicatedly shaped magnetic circuit. However, Hannalla et al.[8],[9] pointed out that the finite element method has weak points for treating a rectangular conductor carrying a uniform current, and for doing rapidly varying currents or voltage such as a surge in a transmission line, or an eddy current induced in an iron core of the electric machine. Therefore, they presented a nodal method, in which acute-angled triangular meshes are used and the physical law is approximated by the principle in the finite difference method. This method is a superior one, but it has the weak point that all usable triangles must be acute-angled ones. Therefore, it is needed to remove the weak point of the nodal method. Recently, we can find the analyses by numerical solutions in consideration of the nonlinearity of the permeability caused by the saturated magnetization curve of the iron core. However, in the conventional two-dimensional analyses, the influence of the hysteresis on behaviors of the magnetic fluxes was not investigated at all.

In this paper, first, there are derived two-dimensional fundamental equations with respect to the vector potential from the Maxwell equations in the electro-magnetic field, where the vector potential is used to obtain easily both the magnetic flux and the eddy current distributions in the electric machine. In order to solve numerically the above fundamental equations, the nodal equation at each node of the triangular meshes, by which the region to be analysed is subdivided, is introduced by a new nodal method which is an improvement over the former nodal method by using any shape of a triangle.

Next, the time derivative of the vector potential in the nodal equation, whicn is needed to calculate the eddy current, is approximated by using the Crank-Nikolson finite difference method.[10] Also, the authors show the numerical method for deriving the nolinear reciprocal permeabilities from the magnetization and the hysteresis curves of the iron cores, in which the Frölich formula is used.

Furthermore, from every nodal equation with the above approximated time derivative and the boundary conditions, the final fundamental nonlinear simultaneous nodal equations are derived. Lastly, the calculaticn processes to solve numerically the nodal equations are shown.

2. Fundamental Equations

The magnetic flux distribution in electric machines can be obained by solving the following Maxwell equations of the electro-magnetic field

$$\mathrm{rot}\boldsymbol{H}=\boldsymbol{J}, \tag{1}$$

$$\mathrm{rot}\boldsymbol{E}=\frac{\partial \boldsymbol{B}}{\partial t}, \tag{2}$$

$$\mathrm{div}\boldsymbol{B}=0, \tag{3}$$

and the additional relations

$$\boldsymbol{B}=\mu\boldsymbol{H}, \tag{4}$$

$$\boldsymbol{J}=\boldsymbol{J}_s+\sigma\boldsymbol{E}, \tag{5}$$

where

$\boldsymbol{B}$: magnetic flux density,
$\boldsymbol{E}$: electric field intensity,
$\boldsymbol{H}$: magnetic field intensity,
$\boldsymbol{J}$: total current density,
$\boldsymbol{J}_s$: current density supplied to conductors of exciting winding,
$\sigma\boldsymbol{E}$: eddy current density induced in iron cores,
μ : permeability which may vary with magnitudes of $\boldsymbol{B}$ and $\boldsymbol{H}$,
σ : conductivity,
t : time.

In the equations, the displacement current and the free-space charge are ignored. Also, we assume that the density of the eddy current induced in the conductors is negligible compared with $\boldsymbol{J}_s$ and the conductivity in each core is uniform.

By using the magnetic vector potential $\boldsymbol{A}$ which is given by

$$\mathrm{rot}\boldsymbol{A}=\boldsymbol{B} \tag{6}$$

so that Eq. (3) may be satisfied, where

$$\mathrm{div}\boldsymbol{A}=0, \tag{7}$$

we can derive

$$\boldsymbol{E}=-\frac{\partial \boldsymbol{A}}{\partial t} \tag{8}$$

from Eq. (2). Then, by Eqs. (2) to (8), Eq. (1) is transformed into the following equation with respect to $\boldsymbol{A}$ and $\boldsymbol{J}_s$

$$\mathrm{rot}(\nu\mathrm{rot}\boldsymbol{A})=\boldsymbol{J}_s-\sigma\frac{\partial \boldsymbol{A}}{\partial t}, \tag{9}$$

where

$\nu=1/\mu$: reciprocal permeability.

If $\boldsymbol{A}$ can be obtained by solving Eqs. (7) and (9), $\boldsymbol{B}$, $\boldsymbol{H}$ and $\boldsymbol{J}$ are evaluated by

$$\boldsymbol{B}=\mathrm{rot}\boldsymbol{A}, \tag{10}$$

$$\boldsymbol{H}=\nu\mathrm{rot}\boldsymbol{A}, \tag{11}$$

$$\boldsymbol{J}=\boldsymbol{J}_s-\sigma\frac{\partial \boldsymbol{A}}{\partial t}. \tag{12}$$

Then, the magnetic flux Φ passing through an arbitrary cross-sectional area S with the contour C is calculated by

$$\Phi=\int_S \boldsymbol{B}\cdot d\boldsymbol{s}=\oint_C \boldsymbol{A}\cdot d\boldsymbol{l}. \tag{13}$$

For simplifying the analysis, let us investigate the two-dimensional flux distribution in an $x-y$ cross-section, which is perpendicular to the rotor axis, of the magnetic circuit in the electric machine. We assume that $\boldsymbol{B}$ and $\boldsymbol{H}$ don't vary in the z direction perpendicular to the cross-section, and that $\boldsymbol{A}$ and $\boldsymbol{J}_s$ have only their respective z components. Then, by using the following relations

$$\boldsymbol{A}=\boldsymbol{k}A(x, y, t)=\boldsymbol{k}A, \tag{14}$$

$$\boldsymbol{J}_s=\boldsymbol{k}J_s(x, y, t)=\boldsymbol{k}J_s, \tag{15}$$

where

$\boldsymbol{k}$: fundamental unit vector in z direction,

Eq. (9) is reduced to the following two-dimensional equation

$$\mathrm{rot}(\nu\mathrm{rot}\boldsymbol{k}A)=\boldsymbol{k}\left(J_s-\sigma\frac{\partial A}{\partial t}\right), \tag{16}$$

where the condition

$$\mathrm{div}\boldsymbol{A}=\mathrm{div}\boldsymbol{k}A=0 \tag{17}$$

must be always satisfied.

Substituting Eqs. (14) and (15) into Eqs. (10) to (13), the following equations are obtained:

$$B_x=\frac{\partial A}{\partial y},\quad B_y=-\frac{\partial A}{\partial x}, \tag{18}$$

$$H_x=\nu\frac{\partial A}{\partial y},\quad H_y=-\nu\frac{\partial A}{\partial x}, \tag{19}$$

$$J=J_s-\sigma\frac{\partial A}{\partial t}, \tag{20}$$

$$\Phi=\oint_C \boldsymbol{k}A\cdot d\boldsymbol{l}=\Delta A l_z, \tag{21}$$

where

B_x and B_y : x and y components of $\boldsymbol{B}$,
H_x and H_y : x and y components of $\boldsymbol{H}$,
J : z component of $\boldsymbol{J}$,
ΔA: difference between vector potentials at some two points on contour C in $x-y$ cross-section of magnetic circuit,
l_z: length of magnetic circuit in z direction.

Next, an equi-vector-potential line shows the corresponding magnetic flux line, because the following relation

$$\frac{dy}{dx}=\frac{B_y}{B_x} \tag{22}$$

is derived from the condition of the derivative

$$dA=\left(\frac{\partial A}{\partial x}\right)dx+\left(\frac{\partial A}{\partial y}\right)dy=-B_y dx+B_x dy=0 \tag{23}$$

on the line.

3. Numerical Solution of Fundamental Equations

3.1. Application of nodal method to basic equations

In order to obtain an approximate numerical solution of Eq. (16) under some given boundary conditions, we use a nodal method as already mentioned.

Now, the domain where Eq. (16) should be solved is subdivided into a large

number of small triangular elements, in which J_s, ν and σ can be assumed to be constant. Then, Eq. (16) is transformed to simultaneous discrete nodal equations with an unknown vector potential at each vertex of every triangular element.

In this section, we study the case where the vector potential is assumed to be expressed by a first order function of position in each element.

At any point (x, y) in a triangular element e_r with nodes i, j and k as shown in Fig. 1, the vector potential $A=A_r(x, y, t)=A_r$ is assumed to be given by the following linear approximation

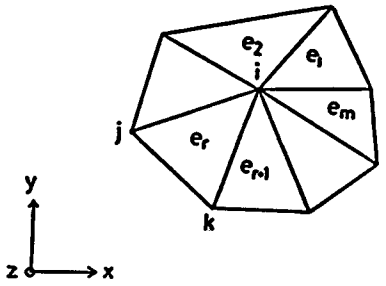

Fig. 1 Node i and adjoining elements holding i in common.

$$A_r=a_r+b_rx+c_ry, \quad r=1, 2, \ldots, m, \tag{24}$$

in which

$$\begin{bmatrix} a_r \\ b_r \\ c_r \end{bmatrix}=\frac{1}{D_r}\begin{bmatrix} a_{ri} & a_{ri} & a_{ri} \\ b_{rj} & b_{rj} & b_{rk} \\ c_{rj} & c_{rj} & c_{rk} \end{bmatrix}\begin{bmatrix} A_{ri} \\ A_{rj} \\ A_{rk} \end{bmatrix},$$

$$a_{ri}=x_{rj}y_{rk}-x_{rk}y_{rj}, \quad b_{ri}=y_{rj}-y_{rk}, \quad c_{ri}=x_{rk}-x_{rj},$$

$$a_{rj}=x_{rk}y_{ri}-x_{ri}y_{rk}, \quad b_{rj}=y_{rk}-y_{ri}, \quad c_{rj}=x_{ri}-x_{rk},$$

$$a_{rk}=x_{ri}y_{rj}-x_{rj}y_{ri}, \quad b_{rk}=y_{ri}-y_{rj}, \quad c_{rk}=x_{rj}-x_{ri},$$

$$D_r=a_{ri}+a_{rj}+a_{rk},$$

A_{rq}, x_{rq} and y_{rq}: A, x and y at node q in e_r, where, $q=i, j, k$,

and we can find the following relations about Fig. 1,

$$A_{ri}=A_i, \quad x_{ri}=x_i, \quad y_{ri}=y_i \text{ for } r=1, 2, \ldots, m,$$

$$A_{rj}=A_{r-1,k}=A_j, \quad x_{rj}=x_{r-1,k}=x_j, \quad y_{rj}=y_{r-1,k}=y_j,$$

$$A_{rk}=A_{r+1,j}=A_k, \quad x_{rk}=x_{r+1,j}=x_k, \quad y_{rk}=y_{r+1,j}=y_k,$$

where

A_q, x_q and y_q: A, x and y at common node q.

From Eqs. (18), (19) and (24), the x and y components B_x, B_y, H_x and H_y of $\boldsymbol{B}$ and

$\boldsymbol{H}$ in element e_r are derived as follows:

$$B_x=\frac{1}{D_r}\sum_{q=i}^{k} c_{rq}A_{rq},\quad B_y=\frac{1}{D_r}\sum_{q=i}^{k} b_{rq}A_{rq}, \tag{25}$$

$$H_x=\frac{\nu_r}{D_r}\sum_{q=i}^{k} c_{rq}A_{rq},\quad H_y=-\frac{\nu_r}{D_r}\sum_{q=i}^{k} b_{rq}A_{rq}, \tag{26}$$

which are constant, where $\nu=\nu_r$ is determined by the relation between $B_r=(B_x^2+B_y^2)^{1/2}$ and $H_r=(H_x^2+H_y^2)^{1/2}$ in e_r. (See Article 3. 3.)

When the expressions similar to Eqs. (24) to (26) are applied to every element, the continuity of the normal component B_n of $\boldsymbol{B}$ on the boundary line of two adjoining elements is maintained. For example, B_n on both sides of the boundary line ik of elements e_r and e_{r+1} in Fig. 1 is given by the following same expression

$$B_n=(A_i-A_k)/\{(x_i-x_k)^2+(y_i-y_k)^2\}^{1/2} \tag{27}$$

where A_i, A_k, x_i, x_k, y_i and y_k are A, x and y at nodes i and k.

On the other hand, the continuity of the tangential component H_t of $\boldsymbol{H}$ on the boundary line can't be expressed by an equation similar to Eq. (27). Hence, to keep the physical law, in our nodal method the above boundary condition for $\boldsymbol{H}$ is replaced by the following Ampēre circuital law

$$\oint_C \boldsymbol{H}\cdot d\boldsymbol{l}=\int_S\left(J_s-\sigma\frac{\partial A}{\partial t}\right)dxdy \tag{28}$$

around each node, where the integral path C is a specific one, for example, as shown by the broken line in Fig. 2, and S is the domain enclosed by C. In the figure, i', j' and k' are the middle points of the three sides $\overline{jk}$, $\overline{ki}$ and $\overline{ij}$, respectively, p is the outer center of element e_r, and the node i is had in common by elements $e_1, e_2, \ldots, e_m$.

From Eqs. (24), (26) and (28) in element e_r, we can derive the following discrete nodal equations

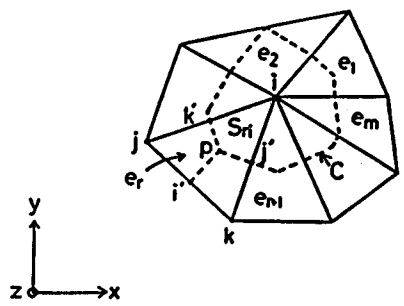

Fig. 2 Integral path C around node i.

$$\int_{k',p,j'} \boldsymbol{Hdl} = \frac{\nu_r}{2D_r} \sum_{q=i}^{k} (b_{ri}b_{rq} + c_{ri}c_{rq}) A_{rq}, \tag{29}$$

$$\int_{i,k',p,j',i} J_s dxdy = J_{sr} S_{ri}, \tag{30}$$

$$\int_{i,k',p,j',i} \left(\sigma \frac{\partial A}{\partial t}\right) dxdy = \sigma_r S_{ri} \frac{\partial A_{ri}}{\partial t} = \sigma_r S_{ri} \frac{\partial Ai}{\partial t}, \tag{31}$$

for node i, where

$$S_{ri} = \frac{1}{16S_r} \{ |b_{ri}b_{rk} + c_{ri}c_{rk}| (b_{rj}^2 + c_{rj}^2) + |b_{ri}b_{rj} + c_{ri}c_{rj}| (b_{rk}^2 + c_{rk}^2) \},$$
$$S_r/4 \leqq S_{ri} \leqq S_r/2. \tag{32}$$

In these equations, J_{sr}, ν_r and σ_r are the values of J_s, ν and σ in element e_r, respectively, and $S_r = D_r/2$ is its area. Here, we must notice that the contributions of $\partial A_j/\partial t$ and $\partial A_k/\partial t$ to the integration result of Eq. (31) were neglected, because those contributions may disturb the resultant eddy current density at node i to approximate the exact one $\sigma \partial A_i/\partial t$. Also, when the element is an obtuse-angled triangle, of which the outer center lies outside itself, as the element e_2 in Fig. 2, we must put $S_{ri} = S_r/4$ or $S_{ri} = S_r/2$ into Eqs. (30) and (31) according to whether the vertical angle of the element at node i is smaller or greater than $\pi/2$.

In this connection, in the conventional nodal method, every element must be an acute-angled triangle. Hence, it is difficult for the conventional nodal method to be applied to a complex field region as in electric machines. Also, the finite element method, in which $S_{ri} = S_r/3$ is substituted into Eq. (30) instead of Eq. (32), has a weak point for treating the rectangular conductor carrying a uniformly distributed current, such as the one in the armature slot of a dc motor.

Next, by using the integration results in Eqs. (29), (30) and (31), and by completing the Ampēre circuital law (Eq. (28)) around node i shown in Fig. 2, the following nodal equation is obtained

$$h_i = f_i - g_i \frac{\partial A_i}{\partial t}, \tag{33}$$

where

$$h_i = \oint_C \boldsymbol{Hdl} = \sum_{r=1}^{m} \frac{\nu_r}{2D_r} \sum_{q=i}^{k} (b_{ri}b_{rq} + c_{ri}c_{rq}) A_{rq} = h_{ii}A_i + \sum_{r=1}^{m} h_{ij}A_{rj}, \tag{34}$$

$$f_i = \int_S J_s dxdy = \sum_{r=1}^{m} J_{sr} S_{ri}, \tag{35}$$

$$g_i = \int_S \sigma dxdy = \sum_{r=1}^{m} \sigma_r S_{ri}, \tag{36}$$

in which

$$h_{ii} = \sum_{r=1}^{m} \frac{\nu_r}{2D_r} (b_{ri}^2 + c_{ri}^2),$$

$$h_{ij}=\sum_{r=1}^{m}\left\{\frac{\nu_r}{2D_r}(b_{ri}b_{rj}+c_{ri}c_{rj})+\frac{\nu_{r-1}}{2D_{r-1}}(b_{r-1,i}b_{r-1,k}+c_{r-1,i}c_{r-1,k})\right\}.$$

In Eq. (34), A_{rq} is the vector potential at node q in e_r, and $A_{ri}=A_i$ is defined in common for $r=1,2,\ldots,m$.

When b_{rq}, c_{rq}, D_r, etc. approach infinitely zero, Eq. (33) may sufficiently approximate the two-dimensional fundamental equation (10) at node i. In this connection, as previously stated, if the terms $\partial A_j/\partial t$ and $\partial A_k/\partial t$ were considered in the integration result in Eq. (31), those terms should disturb the resultant eddy current $g_i\partial A_i/\partial t$ in Eq. (33) to approximate $\sigma\partial A_i/\partial t$ accurately.

3.2. Numerical method for time derivative

In Eq. (33), for node i of $g_i>0$, there is contained the time derivative $g_i\partial A_i/\partial t$. Therefore, in order to numerically solve the equation, we apply the Crank-Nikolson finite difference method to $g_i\partial A_i/\partial t$, by which a sufficiently accurate approximation of $g_i\partial A_i/\partial t$ can be obtained.

When the value of g_iA_i at time t is obtaihed, the value at $t+\Delta t$ is calculated by the following equation

$$(g_iA_i)_{t+\Delta t}=(g_iA_i)_t+\Delta t\left\{\varepsilon_i\left(g_i\frac{\partial A_i}{\partial t}\right)_{t+\Delta t}+(1-\varepsilon_i)\left(g_i\frac{\partial A_i}{\partial t}\right)_t\right\}, \tag{37}$$

where ε_i is a weight factor of the time derivative and $0\leqq\varepsilon_i\leqq1$. From Eqs. (33) and (37), we can get the following nodal equation[10],[11],[12]

$$(g_iA_i+\varepsilon_i\Delta th_i)_{t+\Delta t}=\{g_iA_i-(1-\varepsilon_i)\Delta th_i\}_t+\Delta t\{\varepsilon_i(f_i)_{t+\Delta t}+(1-\varepsilon_i)(f_i)_t\}. \tag{38}$$

Next, for node i of $g_i=0$ and $h_i=f_i$, the nodal equation at $t+\Delta t$ can readily be obtained by putting $g_i=0$ and $\varepsilon_i=1$ in Eq. (38).

3.3. Numerical determination of nonlinear reciprocal permeability

When the element e_r belongs to a region consisting of air or the winding conductors, the reciprocal permeability $\nu=\nu_r$ in Eqs. (26), (29) and (34) is assumed to be equal to the one of the vacuum, namely

$$\nu_r=\nu_0=10^7/(4\pi)\qquad m/H. \tag{39}$$

However, when e_r belongs to an iron core region, ν_r is determined by the nonlinear and multivalued relation between B and H, which are the magnitudes of $\boldsymbol{B}$ and $\boldsymbol{H}$, respectively. This relation is usually given by the $B-H$ curves such as the initial magnetization curve and the hysteresis curve. Here, let us introduce the numerical method for obtaining ν_r corresponding to $B=B_r$ in e_r, where B_r is determined by Eq. (25) as follows

$$B_r=(B_x^2+B_y^2)^{1/2}=\frac{1}{D_r}\{(\sum_{q=i}^{k}b_{rq}A_{rq})^2+(\sum_{q=i}^{k}c_{rq}A_{rq})^2\}^{1/2}. \tag{40}$$

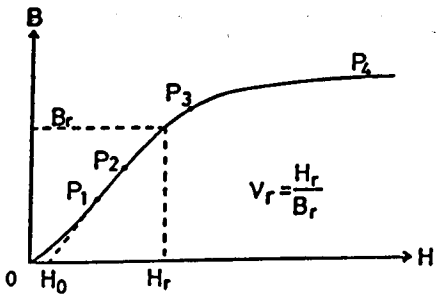

Fig. 3 Frölich formula for obtaining reciprocal permeability ν_r by initial magnetization curve.

(1) Derivation of ν_r from magnetization curve

When $B=B_r$ increases from an initial unmagnetized value, the $B-H$ curve is expressed by the initial magnetization curve $OP_1P_2P_3P_4$, as shown in Fig. 3. Then, $H=H_r$ corresponding to B_r is found by the curve, and sequentially the exact value $\nu_r=H_r/B_r$ can be obtained. However, this process is too complicated to be used for practical calculation.

In our numerical method, the following Frölich formula

$$B=\frac{H-H_0}{\eta+\xi(H-H_0)} \tag{41}$$

is adopted to obtain the approximate value of ν_r, where η, ξ and H_0 are the coefficients determined by the $B-H$ curve. By applying Eq. (41) to the segment $P_1P_2P_3$ of the curve in Fig. 3, ν_r is expressed by

$$\nu_r=\frac{H_r}{B_r}=\frac{\eta}{1-\xi B_r}+\frac{H_0}{B_r}, \qquad B_1\leqq B_r\leqq B_3, \tag{42}$$

where

$$\eta=\frac{(B_1-B_2)(B_2-B_3)(B_3-B_1)(H_1-H_2)(H_2-H_3)(H_3-H_1)}{B_1B_2(H_1-H_2)+B_2B_3(H_2-H_3)+B_3B_1(H_3-H_1)}, \tag{43}$$

$$\xi=\frac{B_1(H_3-H_2)+B_2(H_1-H_3)+B_3(H_2-H_1)}{B_1B_2(H_1-H_2)+B_2B_3(H_2-H_3)+B_3B_1(H_3-H_1)}, \tag{44}$$

$$H_0=\frac{B_1B_2H_3(H_1-H_2)+B_2B_3H_1(H_2-H_3)+B_3B_1H_2(H_3-H_1)}{B_1B_2(H_1-H_2)+B_2B_3(H_2-H_3)+B_3B_1(H_3-H_1)}, \tag{45}$$

in which

B_i and H_i: B and H at P_i, $i=1, 2, 3$.

By the above process, we can get ν_r for any value of B_r on the $B-H$ curve. In this connection, when B_r as given by Eq. (40) is estimated over the saturation value

of B, for example $B_r>B_4$, ν_r is calculated by $\nu_r=H_4/B_4$, where $B=B_4$ and $H=H_4$ at point P_4.

(2) Derivation of ν_r from hysteresis curve

When B decreases from point P_1 on the initial magnetization curve, the $B-H$ curve is expressed by the hysteresis segment $P_1P_2P_3P_4$, as shown in Fig. 4. Now, ν_r for $B=B_r$ on the one $P_1P_2P_3$ is obtained by substituting the values of B and H at the three points P_1, P_2 and P_3 into Eqs. (42) to (45) as follows:

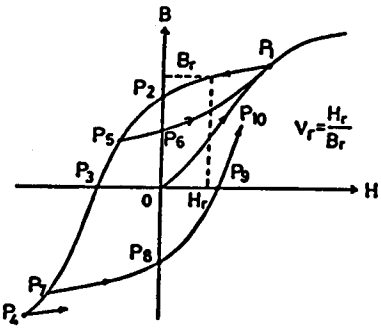

Fig. 4 Application of Frölich formula to hysteresis curve for obtaining reciprocal permeability ν_r

$$\nu_r=\frac{\eta}{1-\xi B_r}+\frac{H_0}{B_r}, \tag{46}$$

where

$$\eta=\frac{(B_2-B_1)(H_1-H_3)H_3}{B_1B_2H_1}: \text{ equal to slope } dB/dH \text{ at } P_3, \tag{47}$$

$$\xi=\frac{B_1H_3+B_2(H_1-H_3)}{B_1B_2H_1}, \tag{48}$$

$$H_0=H_3<0,$$

in which

B_i and H_i: B and H at P_i, $\quad i=1, 2, 3.$

In this connection, $B=B_2$ at P_2 and $H=H_3$ at P_3 are called the residual magnetism and the coercive force, respectively.

When $B=-B_r$ becomes negative on the hysteresis segment P_3P_4, η and H_0 keep the values given by Eqs. (47) and (49), and so only the value of ξ in Eq. (46) is replaced by

$$\xi=\frac{H_4-H_3-\eta B_4}{B_4(H_4-H_3)}, \tag{50}$$

where

$$B_4=-B_1 \text{ and } H_4=-H_1\text{: } B \text{ and } H \text{ at } P_4.$$

Next, let us consider ν_r in the case where B stops decreasing at some point on the hysteresis segment and inversely increases from that point. When $B=B_r$ increases from point P_5 on the segment $P_1P_2P_3$ in Fig. 4, $B=B_6$ at point P_6 is first evaluated under the assumption that the line segment $\overline{P_5P_6}$ is parallel to the one $\overline{P_1P_2}$, so that η, ξ, H_0 and ν_r may be obtained by using the values of B and H at the three points P_5, P_6 and P_1 as well as in Eqs. (42) to (45).

When $B=B_r$ increases from point P_7 on the segment P_3P_4, the segment $P_7P_8P_9P_{10}$ is evaluated by Eq. (41) under the assumption that the segment $\overline{P_7P_8}$ is parallel to $\overline{P_1P_2}$ and dB/dH at P_9 is equal to the one at P_3. Then, ν_r for $B=B_r$ is obtained by a computation process similar to the one given by Eqs. (46) to (50).

3.4. Basic nodal equations considering boundary conditions

Here, let us introduce the nodal equation for node i which exists on the boundary line, as shown in Fig. 5 (a) and (b). On a boundary line where the normal component B_n of B is zero, the relation $A=A_i=A_k$, which doesn't depend on x and y, is obtained by substituting $B_n=0$ into Eq. (27). Then, the nodal equation (38) for i is rewritten as follows:

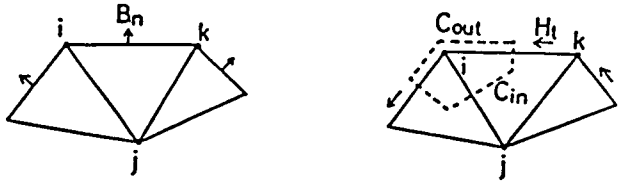

(a) $B_n=0$ (b) $H_t=0$

Fig. 5 Typical boundary conditions.

$$\Delta t(h_i)_{t+\Delta t}=\Delta t(f_i)_{t+\Delta t}, \tag{51}$$

where

$$h_i=A_i,\quad g_i=0,\quad \varepsilon_i=1,$$

$f_i=A_c$: vector potential given on boundary line.

On another boundary where the tangential component H_t of $\boldsymbol{H}$ is zero, the nodal equation for node i is derived from integrating Eq. (28) in a circuital integral region given by the broken line in Fig. 5 (b), where C_{out} and C_{in} are the outside and the inside paths of our integral region, respectively. In this case, the line integration along C_{out} vanishes because of $H_t=0$, and that along C_{in} is easily carried out by Eqs.

(29) and (34). As a result, we can get a discrete nodal equation similar to Eq. (38), where $f_i=0$ and $g_i=0$ because $J_s=0$ and $\sigma=0$ near the boundary line.

Finally, from Eqs. (38) and (51), the basic nonlinear simultaneous nodal equations for all nodes are readily derived as follows:

$$([G]+\Delta t[\varepsilon][H])[A]_{t+\Delta t}=\{[G]-\Delta t([U]-[\varepsilon])[H]\}[A]_t + \Delta t\{[\varepsilon][F]_{t+\Delta t}+([U]-[\varepsilon])[F]_t\}, \tag{52}$$

in matrix form, where

$$[A]=\begin{bmatrix} A_1 \\ A_2 \\ \vdots \\ A_i \\ \vdots \\ A_n \end{bmatrix},\quad [F]=\begin{bmatrix} f_1 \\ f_2 \\ \vdots \\ f_i \\ \vdots \\ f_n \end{bmatrix},\quad [G]=\begin{bmatrix} g_1 & 0 & \cdots & & & 0 \\ 0 & g_2 & \cdots & & & 0 \\ \vdots & & & & & \vdots \\ 0 & & & g_i & & 0 \\ \vdots & & & & & \vdots \\ 0 & & & & & g_n \end{bmatrix},$$

$$[H]=\begin{bmatrix} h_{11} & h_{12} & \cdots & & h_{1n} \\ h_{21} & h_{22} & \cdots & & h_{2n} \\ \vdots & & & & \vdots \\ h_{i1} & & h_{ii} & & h_{in} \\ \vdots & & & & \vdots \\ h_{n1} & & & & h_{nn} \end{bmatrix},\quad [\varepsilon]=\begin{bmatrix} \varepsilon_1 & 0 & \cdots & & 0 \\ 0 & \varepsilon_2 & \cdots & & 0 \\ \vdots & & & & \vdots \\ 0 & & \varepsilon_i & & 0 \\ \vdots & & & & \vdots \\ 0 & & & & \varepsilon_n \end{bmatrix}.$$

In these equations,

n : total nuwber of nodes,

$[A]$: row matrix constructed with unknown vector potentials at all nodes,

$[F]$: row matrix derived from f_i in Eq. (35) and $f_i=A_e$ in Eq. (51),

$[G]$: diagonal coefficient matrix derived g_i in Eq. (36) and $g_i=0$ in Eq. (51),

$[H]$: nonlinear and sparse coefficient matrix, in which coefficients h_{ij} (i and $j=1, 2, \ldots,$ n) are derived from coefficients for A_i and A_{r_j} in Eq. (34), and $h_{ii}=1$ and $h_{ij}=0$ for $i\neq j$ in Eq. (51),

$[\varepsilon]$: diagonal matrix constructed with ε_i in Eq. (38) and $\varepsilon_i=1$ in Eq. (51),

$[U]$: unit matrix.

By numerically solving Eq. (52), the transient values of $[A]$ at all nodes are obtained. Also, by putting $\Delta t=1$, $g_i=0$ and $\varepsilon_i=1$ for $i=1$ to n in Eq. (52), the values of the vector potential in the steady state, where the eddy current vanishes, can be obtained.

3.5. Numerical calculation process

In Fig. 6, there is shown the flow chart of a calculation process for numerically solving the nonlinear simultaneous equation (52) and obtaining the transient responses of the vector potentials $[A]$ for the change of the exciting current. The calculation process is as follows:

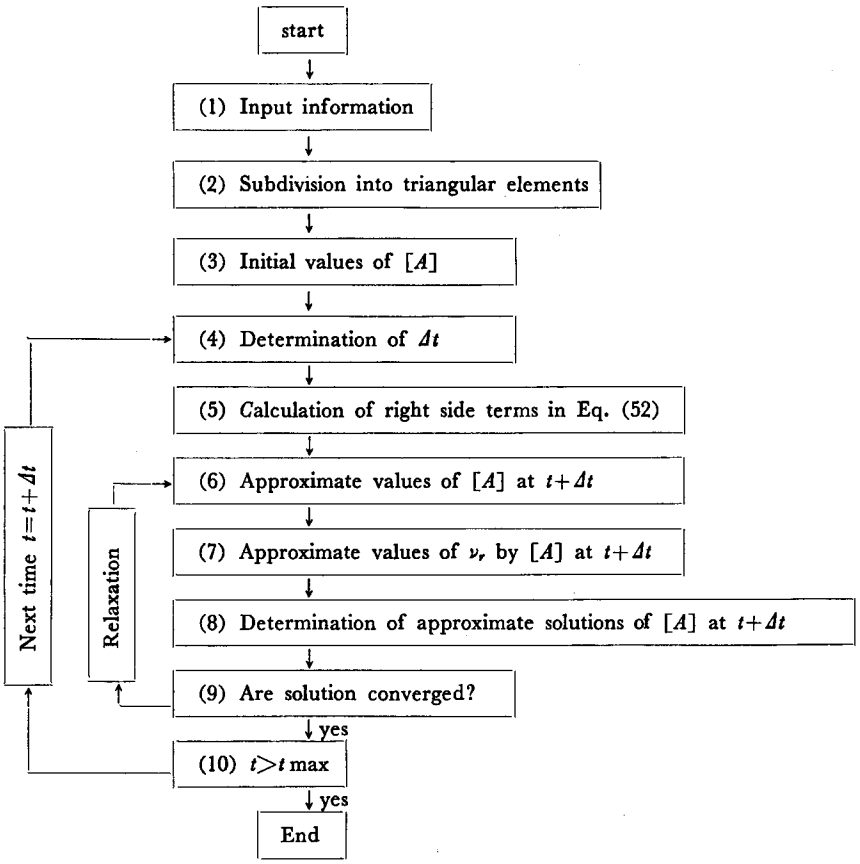

Fig. 6 Flow chart of calculation process for solving Eq. (52).

(1) We provide the input information about the shape, the dimensions, the structural materials, etc. of the machine, and the boundary conditions.

(2) The analysed domain is subdivided into a large number of triangular elements.

(3) We provide the initial values of the vector potentials $[A]$ at all nodes of the elements.

(4) The supplied current density J_s at time $t+\Delta t$ is calculated by dividing the current in the conductor of the exciting winding by its cross-sectional area, where Δt is determined small enough to obtain the accurate transient responses of $[A]$.

(5) By using the already determined $[A]_t$ and J_s, the calculation of the right side terms of Eq. (52) is carried out.

(6) The approximate values of $[A]_{t+\Delta t}$ are estimated.

(7) By using the approximate values of $[A]_{t+\Delta t}$, the nonlinear reciprocal permeabilities ν_r's in elements within iron core are calculated by the method shown in Article

3. 3.

(8) By solving Eq. (52), the approximate solutions of $[A]_{t+\Delta t}$ are determined.

(9) The processes (6) to (8) are iterated till the convergence of $[A]_{t+\Delta t}$ is ascertained. In this connection, the approximate values in a following iteration are evaluated by the successive relaxation method, by which repetition time can be fairly decreased[12].

(10) The above processes (4) to (9) for the next successive time $t=t+\Delta t$ are repeated till $t=t_{max}$, where t_{max} is the calculation interval needed to investigate the transient response of $[A]$.

Next, when the transitional change of $[A]$ by the one of the current density J_s proportional to the exciting current is calculated, the transitional distribution of the magnetic flux can be shown by the equi-vector-potential lines, namely the flux lines. The distribution of the flux density is derived from Eq. (25). Also, by Eqs. (33) and (36). the eddy current density in the iron core can be numerically evaluated

$$-\frac{g_i}{S_i}\frac{\Delta A_i}{\Delta t}=-\frac{\sum_{r=1}^{m}\sigma_r S_{ri}}{S_i}\frac{\Delta A_i}{\Delta t}, \tag{53}$$

where

ΔA_i: increment of $A=A_i$ at node i during Δt,

$S_i=\sum_{r=1}^{m}S_{ri}$.

Furthermore, the transient response of the magnetic flux Φ in a cross-section of the magnetic circuit can easily be calculated by Eq. (21).

4. Conclusion

The main results obtained by the investigation of the numerical solution in this paper are as follows:

(1) By using the magnetic vector potential, the two-dimensional fundamental equations, by which the transient flux distribution in electric machines can be analysed, were derived from the Maxwell equations for the electro-magnetic field. In the equations, the eddy currents induced in iron cores and the nonlinear permeability were considered.

(2) The nodal method, which is known as the finite difference method using triangular elements, was applied to solve the two-dimensional equations, and the nodal equation at the node of the element was introduced.

(3) The time derivative $g_i\partial A_i/\partial t$ contained in the nodal equation was approximated by the Crank-Nikolson finite difference method, and then the final discrete nodal equation was introduced.

(4) The numerical method for deriving the nonlinear reciprocal permeability ν_r

from the magnetization and the hysteresis curves of iron cores was obtained by using the Frölich formula.

(5) The nodal equations considering the basic boundary conditions concerning the magnetic flux density and the magnetic field intensity were obtained. Furthermore, the nonlinear simultaneous nodal equations for all nodes were introduced.

(6) The calculation processe to solve the nonlinear simultaneous equation was shown. In the process, the successive relaxation method should be used for decreasing the repetition time required to solve the equations.

By using a numerical solution, the transitional change of the vector potential due to the abrupt change of the exciting current in the electric machine can be calculated. Then, the transitional distribution of the magnetic flux can be shown by the equi-vector-potential lines, namely the flux lines. Also, the distributions of the flux density, the eddy current density, etc. can be numerically evaluated. Furthermore, the transient response of the magnetic flux in a cross-section of the magnetic circuit can easily be obtained.

References

1) Rüdenberg, R.: 'Transient Performance of Electric Power Systems,' MaCgrow-Hill, New York, pp. 106-133 (1950).
2) Švajcr, J. : 'Transient Phenomena in Magnetic Circuits Having Components of Solid Ferromagnetic Material, I. E. E' E. Trans. on MAG, Vol. MAG-10, No. 1, pp. 54-59 (1974).
3) Sakabe, S., T. Nomura, and M. Iwamoto: 'Delay of Interpole Flux of DC Machines due to the Existence of Liner,' J. I. E. E. J., Vol. 97-B, No. 5, pp. 279-286 (1977).
4) Wagner, C. F.: 'Transients in Magnetic Systems,' Electrical Engineering, Vol. 53, No. 3, pp. 418-425 (1934).
5) Ahmed, S. V., and E. A. Erdelyi: 'Flux Distribution in DC Machines On-Load and Overloads,' I. E. E. E. Trans. on PAS, Vol. PAS-85, No. 9, pp. 960-966 (1966).
6) Erdelyi, E. A., E. F. Fuchs, and D. H. Binkley: 'Nonlinear Magnetic Field Analysis of DC Machines-Part III, Equipotential Plots Drawn by Computer,' I. E. E. E. Trans. on PAS, Vol. PAS-85, No 7, pp. 1565-1583 (1970).
7) Chari, M. V. K., and P. Silvester: 'Finite-Element Analysis of Magnetically Saturated D-C Machines,' I. E. E. E. Trans. on PAS, Vol. PAS-90, No. 8, pp. 2362-2372 (1971).
8) Hannalla, A. Y., and D. C. Macdonald: 'A Nodal Method for the Numerical Solution of Transient Field Problems in Electrical Machines, I. E. E. E. Trans. on MAG, Vol. MAG-11, No. 5, pp. 1544-1546 (1975).
9) Dermerdash, N. A.: 'A New Approach for Determination of Eddy Current and Flux Penetration in Nonlinear Ferromagnetic Materials,' I. E. E. E. Trans. on MAG, Vol. MAG-10, No. 3, pp. 682-685 (1974).
10) Smith, G. D. (Translated by Y. Fujikawa) : 'Numerical Solution of Partial Differential Equation,' 2nd ed., Science sha &, Tokyo, pp. 17-18 (1975).
11) Ando, T., and J. Umoto: 'Analysis of Transient Response of Magnetic Flux in Nonlinear Magnetic Circuit,' J. I. E. E. J., Vol. 100-B, No. 8, pp. 492-498 (1980).
12) Ando, T., and J. Umoto: 'Analysis of Transient Response of Magnetic Flux in Nonlinear Magnetic Circuit,' Memoirs of the Faculty of Engineering, Kyoto Uhiversity, Vol. 42, Part 3, pp. 243-257 (1980).